The Bartlett School of Environment, Energy and Resources

UCL Institute for Sustainable Heritage

UCL Candidate Code: YCWP6

Module Code: BENV0064

Module Title: SEAHA – Research Methodology

Coursework Title: Salt and Vinegar Minerals: a proof-of-concept experiment

Module Leader: Josep Grau-Bove

Date: 14.01.2019

Word Count: 4000; 3771

By submitting this document, you are agreeing to the Statement of Authorship:

I/We certify that the attached coursework exercise has been completed by me/us and that each and every quotation, diagram or other piece of exposition which is copied from or based upon the work of other has its source clearly acknowledged in the text at the place where it appears.

I/We certify that all field work and/or laboratory work has been carried out by me/us with no more assistance from the members of the department than has been specified.

I/We certify that all additional assistance which I/we have received is indicated and referenced in the report.

Please note that penalties will be applied to coursework which is submitted late or which exceeds the maximum word count. Information about penalties can be found in your Course Handbook which is available on Moodle:

- ***Penalties for late submission: https://moodle.ucl.ac.uk/course/view.php?id=41523&section=27***
- ***Penalties for going over the word count: https://moodle.ucl.ac.uk/course/view.php?id=41523&section=26***

In the case of coursework that is submitted late and is also over length, then the greater of the two penalties shall apply. This includes research projects, dissertations and final reports.

Executive Summary

The purpose of this experiment was to trial accelerated aging conditions and methods of analysis to determine relevance and applicability for larger-scale experimentation. Calcite and pyrite samples were exposed to a carbonyl-water-salt solution of acetic acid, water, and sodium chloride to replicate a humid, corrosive environment. Acetic acid concentration, heat, and a moderately high humidity accelerated the deterioration processes. These conditions proved too extreme, yet this experiment identified aspects of the procedure that could be improved to better reflect museum conditions.

- A salt solution is not viable as a means to create humid environments, as it adds an additional, usually unwanted salt contamination.
- Colorimetry of minerals with uneven surfaces proves to introduce error, producing unreliable results.
- Multiple forms of compositional analysis (i.e. x-ray diffraction and Fourier transform infrared spectroscopy) are needed to better determine probable reaction products.

In conclusion, more realistic aging conditions should be used to better correlate experimental with real-time data.

Introduction

Acetic acid is one of many common indoor pollutants in museums (Waller et al. 2000; Grzywacz 2006). It is emitted from wood, some adhesives, and additional housing materials used for the display and storage of collections (Waller et al. 2000: 3; Grzywacz 2006: 11-12, 101-103). This acid affects namely cupperous and plumbous metals (Thickett 1997; Tétreault et al. 2003; Grzywacz 2006: 11-12, 101-103) as well as calcereous materials, such as cermaics, shells, and stone (Tennent & Baird 1985; Grzywacz 2006: 11-12, 101-103; Caracanhas Cavallari et al. 2014). Literature discussing the acid's effect on the later is limited, and within such texts there is little to no direct mention of how it specifically affects calcerous minerals.

The following accelerated aging experiment was devised to begin exploring the effects of common gaseous pollutants on minerals, starting with one pollutant (acetic acid) and two well-documented minerals (calcite and pyrite) in a simplistic vessel. Quantifable data and groundbreaking insights were not the objectives for this experiment. Rather, it was performed as a proof-of-concept; to test the feasability and appropriateness of the test conditions and methods for later application at a larger scale.

Experimental Procedure

Glassware was first rinsed with hot water then acetone to remove any unwanted residues. Samples were likewise degreased with acetone then weighed on a digital balance (Sartorius CP42025) with a precision of ± 0.01g. Colour and lightness measurements of all samples were determined with a spectrophotometer (Konica Minolta CM-700d) using the L*a*b* colour space. Photographs and observations – with and without a stereomicroscope (Leica MSV269 and Keyence VH-250L) – were also taken for all specimens.

Referencing a previous experimental procedure (Tétreault et al. 2003), glass deterioration vessels were similarly created to expose samples of calcite and pyrite to acetic acid vapour within a humid environment. This was achieved through the use of a carbonyl-water-salt mixture. Five sets of each mineral were exposed to a humid environment containing an 80% solution of acetic acid in deionised water (C1-5 & P1-10), and one of each exposed to just a humid environment (C10 & P11-12). Remaining samples were used as controls (C6-9 & P13-19).

Approximately 16.6 g of sodium chloride (NaCl) were used per vessel to generate a relative humidity of 74.5±0.3% (Greenspan 1977; Omega n.d.). This was mixed with 20ml of the acetic acid solution. The samples were placed inside or rested atop a 10ml beaker (Fig. 1). This method was chosen over suspending the sample from the lid, as any material used to do so would dissolve and or prove to be an additional variable to the experiment through reaction with acetic acid.

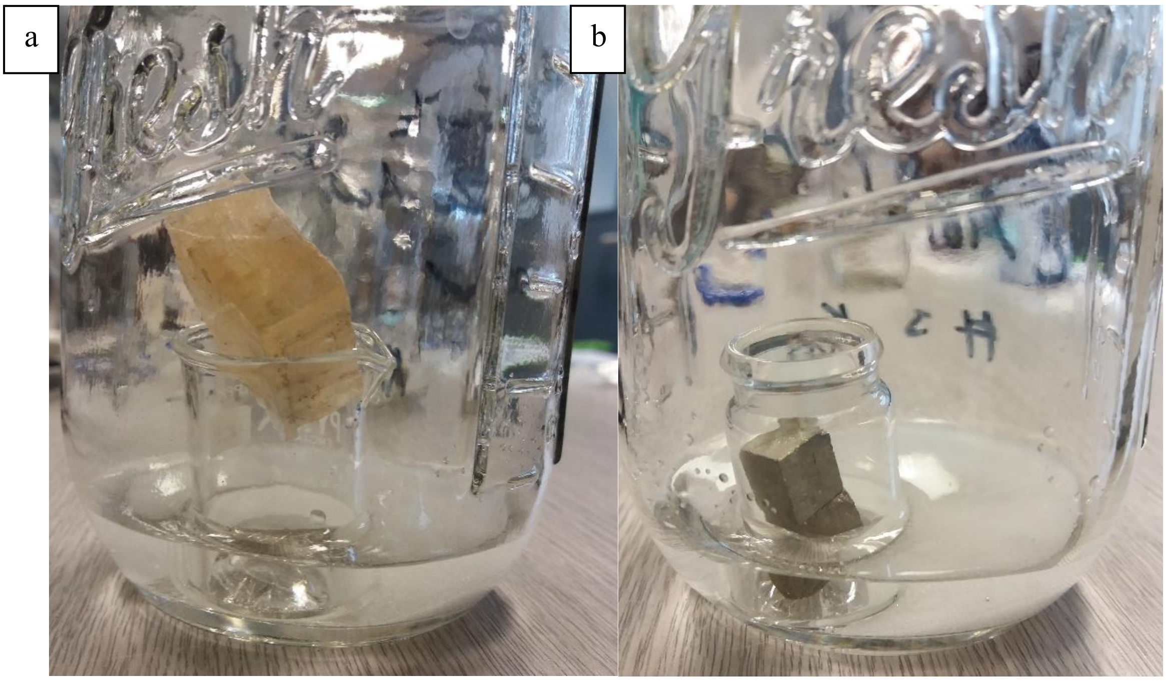

Figure 1. Jar set up: a.) calcite samples rested within the mouth of a 10ml beaker, while b.) 2 pyrite cubes were placed in similarly sized glass vials. These containers were then added to 500ml jars containing 20ml of solution.

The salt solution and samples were then placed within a 500ml glass jar covered with a watch glass. Watch glasses were used to produce loose seals, not only to replicate the imperfect seals of museum housing, but also to ensure that pressure within the vessel did not significantly build up to the point where they exploded. The containers were kept in a Genlab OV/125/F/DIG oven set to 60°C (Fig. 2) for 7 days and checked at 24 hour intervals, save over the weekend (days 4 & 5). Solutions were topped up by 10 or 20 ml on days 2, 3, and 6.

Upon removal from the oven on day 8, samples were documented in the same fashion as before deterioration; observed, weighed, photographed, and took colorimetry measurements. Scanning electron microscopy with electron dispersive x-ray analysis (SEM-EDX; Jeol 5910 & INCA 300) was also employed - with a beam voltage of 15kV and current of 1nA - to view crystal morphology and identify composition.

Results

Accelerated Aging

The construction of the vessels was successful, as they were able to maintain a humid environment (indicated by the condensation on their inner walls upon removal to room temperature from the oven), keep the samples out of the liquid solution, and expose most sample faces to the vapour.

Calcite samples 1-5 began to effloresce within 24 hours, with efflorescence visible on most faces after 48 hours. At this time, C3 split (Fig. 2b) along a cleavage front with gentle handling for photography. Samples became more friable over the duration of the experiment; small pieces of efflorescence and calcite would flake and crumble off the samples (Fig. 2d), especially with handling. Splits and cracks were also found on most of the samples after day 6. These fronts were where the samples first broke with mild shock (i.e. placing on a table) or with handling after 7 days of exposure. After removal from the oven on day 8, C1-5 disintegrated with minor stresses and shocks created by their transportation to various laboratories for analysis. C10, however, changed little as the experiment progressed.

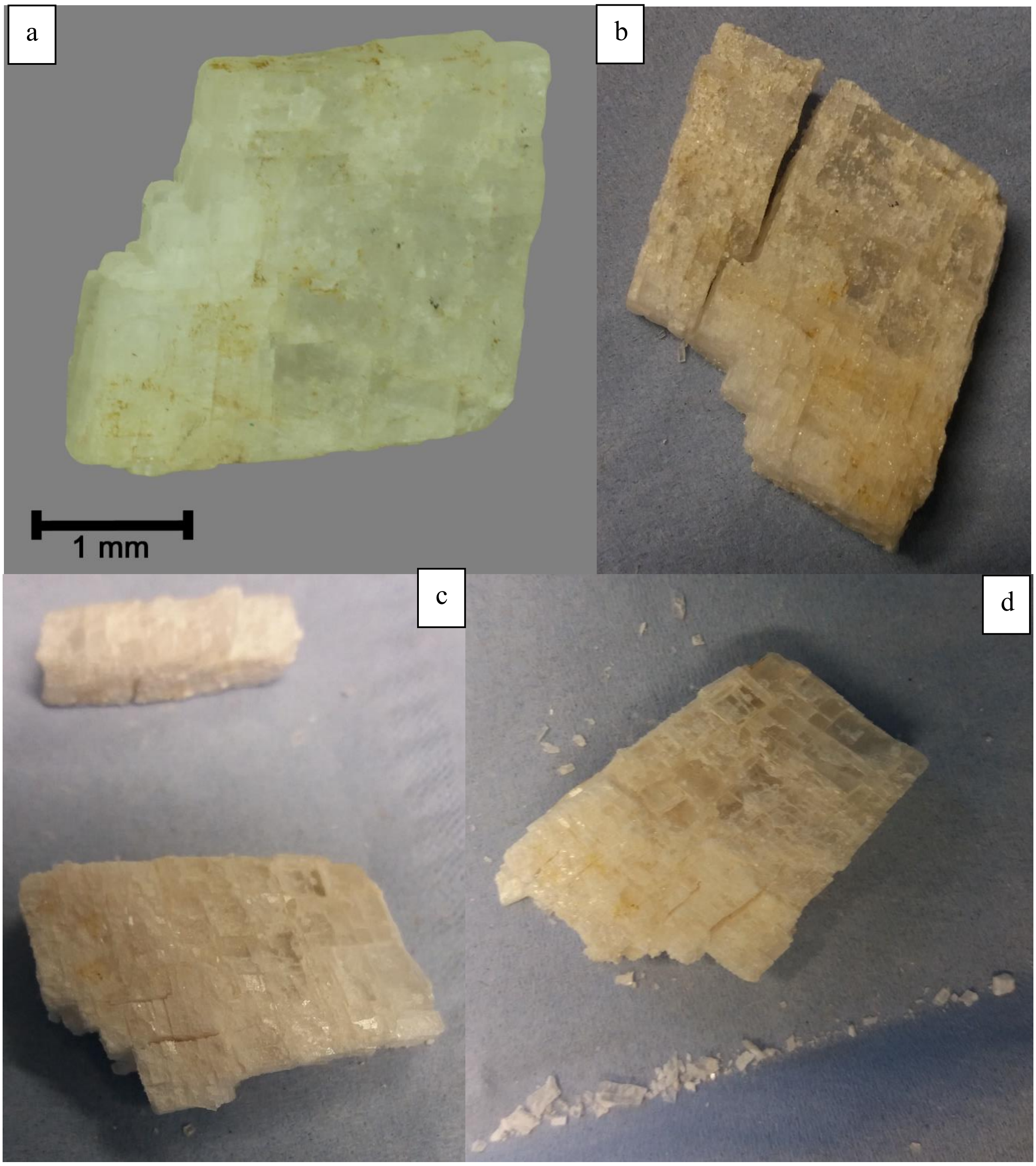

Figure 2. Calcite Sample 3 a.) before, b.) day 2, c.) day 6, & d.) end of experiment. This sample was the first to break and show signs of friability.

Throughout the experiment, the 12 pyrite samples appeared to have been minimally affected by the accelerated conditions, if at all. At best, they seemed duller (Fig. 3b), yet slightly more golden when removed on day 8. These visual changes were more noticeable with samples 11 & 12.

Figure 3. Pyrite sample 1 (50x magnification) a.) before & b.) after experimentation. The only visual difference is the duller appearance of the latter. Rusty oxidation products can be seen on the right side of the sample.

Weight Gain

Calcite samples 1-5 were the only samples to experience significant weight change, ranging from 0.16 – 0.40 g (Appendix B). These samples were weighed in their polybags to mitigate further losses due to their friable nature. Some of the other samples experienced a change in weight by ±0.02, but these were considered to be within acceptable reading error.

Colorimetry

While appearing useful, colorimetry failed to produce reliable results due to an unidentifiable error range. Error was introduced through the uneven nature of the minerals. The samples were also a bit too small to sufficiently cover the reading area of the equipment. These two factors led to the device-emitted light to escape from the detection area and possibly skewing the readings, despite performing an average of at least three readings for each sample. As a result, the data produced (Appendix C) has limited reliability with questionable utility. The ΔE^*ab values (Table 1) – or the total value of change expressed as a single number – exemplifies this, as the values vary widely with no trend expressed.

*Table 1. ΔE*ab values (SCI / SCE) of deteriorated samples.*

Sample #	Calcite	Pyrite
1	28.39 / 35.48	22.81 / 22.76
2	14.03 / 16.34	26.68 / 27.15
3	17.04 / 21.08	7.27 / 7.16
4	18.41 / 20.47	3.03 / 2.93
5	29.38 / 32.64	34.98 / 35.73
6	16.02 / 18.65	0.78 / 0.60
7	6.94 / 6.87	8.14 / 8.10
8	7.34 / 7.59	29.29 / 30.23
9	9.46 / 11.33	19.69 / 19.94
10	7.64 / 10.81	5.08 / 4.95
11	-	23.14 / 23.01
12	-	23.31 / 23.98

Microscopy & Electron Dispersive X-ray Spectroscopy (EDS)

Calcite samples 1-5 produced needle-like, flowering crystals (Fig. 4) when viewed under a stereomicroscope. Yet when viewed with the SEM, most crystals produced on the calcite substrates are comparable to those of aragonite and calcite (Hu & Deng 2004: Fig. 2,5; Rautaray et al. 2004: Fig. 4; Liu et al. 2010: Fig. 6; Fu et al. 2012: Fig. 3), with rod, platelet, and nodule formations (Fig. 5). All EDS spectra contain calcium, carbon, and oxygen, while chloride is present in the majority. Yet there is no correlation between crystal form and chloride content. Thus, it cannot be determined whether the chloride detected is part of the crystal formation or is a surface contaminant.

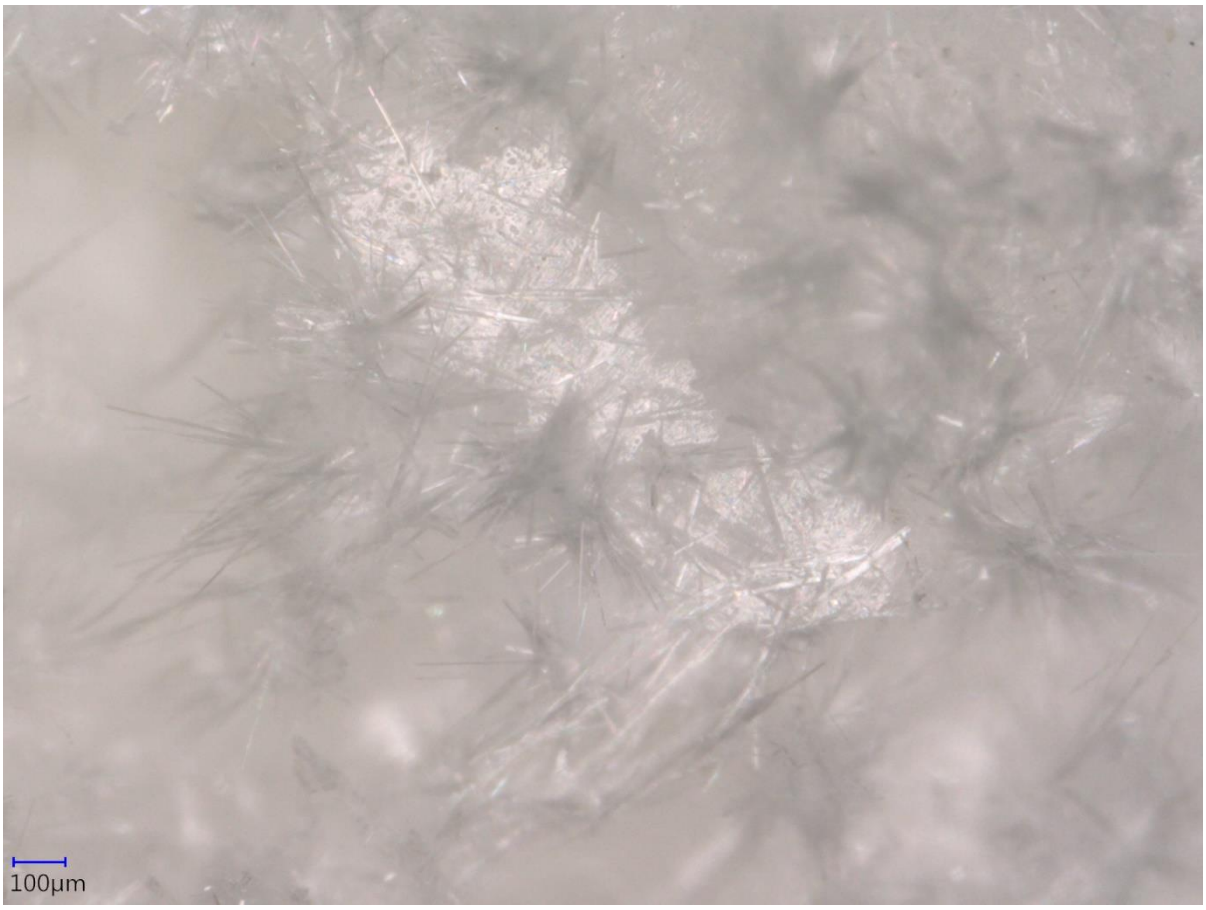

Figure 4. Calcite sample 1 at 150x magnification, showing the flowering, needle-like crystals.

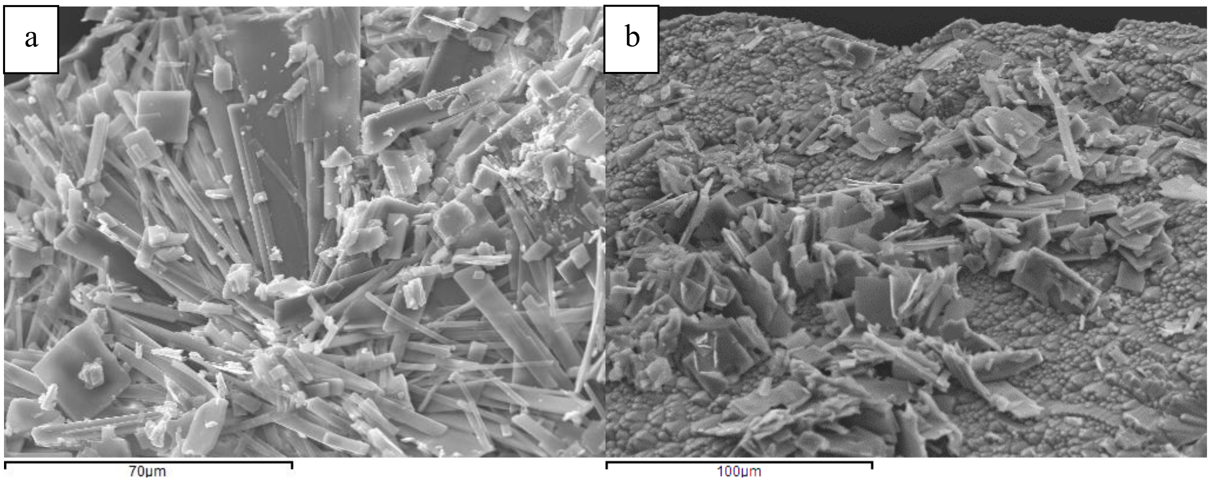

Figure 5. SEM micrographs of a calcite crystals from sample 2. EDS spectra from a.) included peaks of Cl, which are not present on b.), despite some similar looking crystal formations.

Under a stereomicroscope, little difference was noted (Fig. 3) on the pyrite samples after the experiment. However, there were microscopic changes detectable by SEM. Almost the entire surface of the pyrite samples examined (1, 3, & 12) was speckled (Fig. 6) with small, flowering crystals (Fig. 8a) that disrupt the surface, increase porosity, and cause minute cracks and redeposition of pyrite crystals (Fig. 7). EDS spectra of these sites included peaks of iron, sulphur, oxygen, sometimes sodium, and minute quantities of common impurities (Ni, Co, As, Zn; Mindat.org 2019). Chloride mainly appears associated with sodium in spectra from sample 12, but is not seen elsewhere.

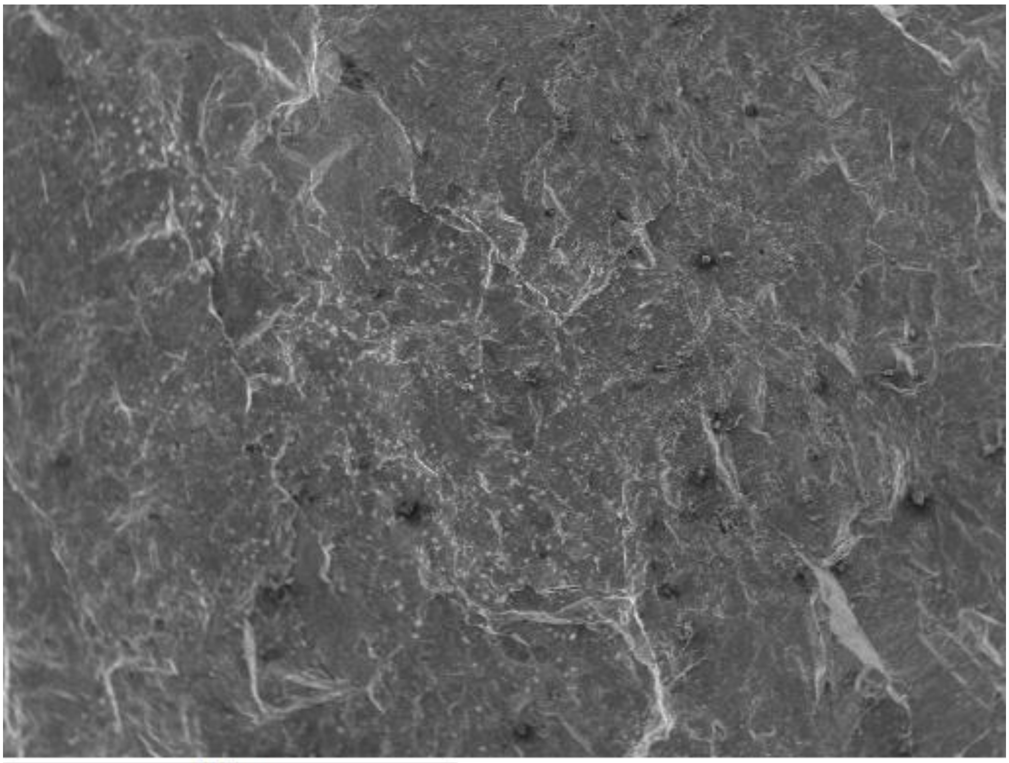

Figure 6. SEM micrograph depicting the topography of P1. The white specks are flowering crystals (Fig. 8a).

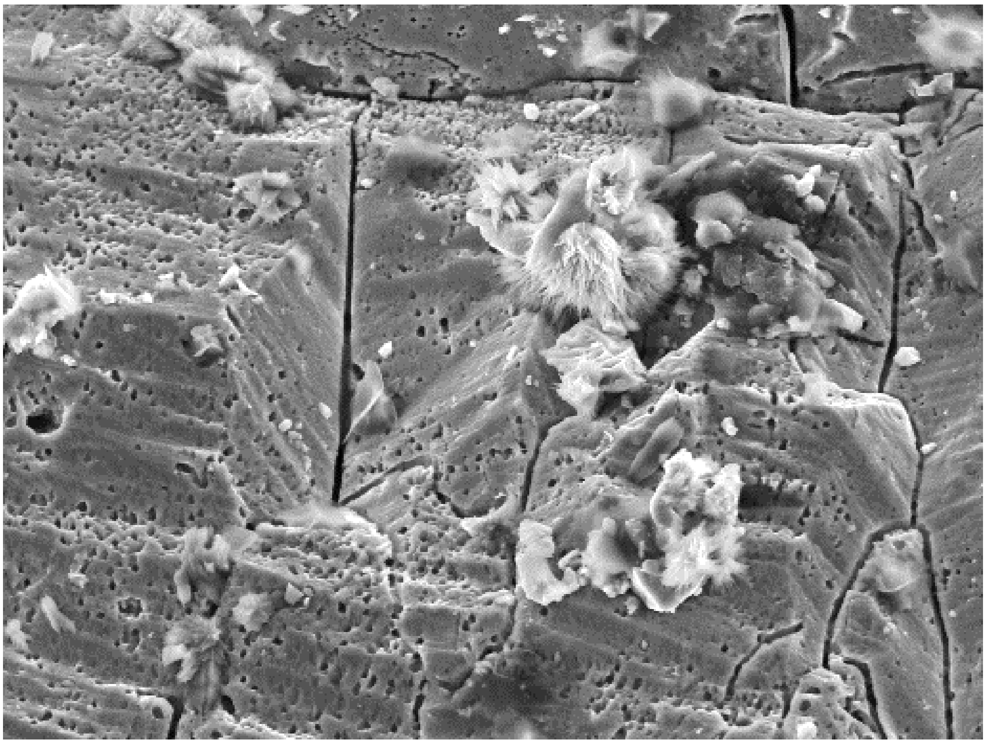

Figure 7. SEM micrograph from P3, depicting cracks, pores, redeposited pyrite, and flowering, furry crystals.

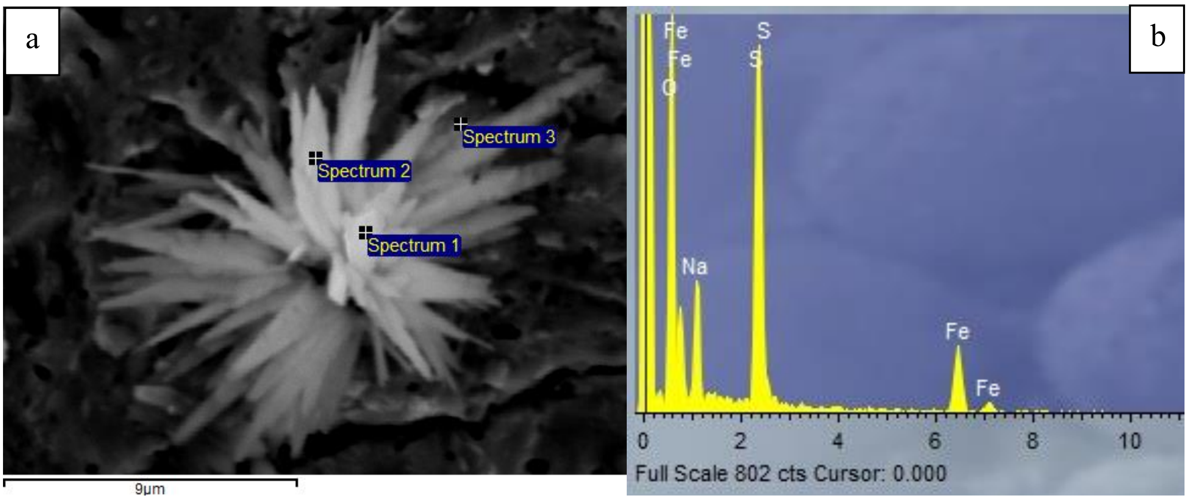

Figure 8. a.) Micrograph of a flower crystal from P1 with spectra sites. b.) Spectrum 1, revealing a significant Na presence.

Discussion

The deterioration of the calcite samples appeared to similar to Bynesian decay: white efflorescence, crumbling, fracture. The detection of chloride by EDS suggests it has a role in the reaction, which some authors (Tennent & Baird 1985; Caracanhas Cavallari et al. 2014) imply is necessary for Bynesian decay to occur. Yet how significant is this role? Is it critical for the reaction to occur? When comparing C10 to C1-5, the primary reactant for the latter seems to be acetic acid. Yet sodium chloride could play a role in initiating the reaction. It is difficult to confirm this, as well as to determine the exact reaction pathways and products, due to the extremity of aging conditions and lack of additional compound analysis (i.e. Fourier Transform Infrared (FT-IR) or Raman spectroscopy), as the latter were inaccessible during the time constraints of the experiment. However, one could anticipate the efflorescence created by this experiment to comprise of various acetate and chloride salts, oxides, and or carbonates.

In contrast, it was surprising to see minimal reactivity in the pyrite samples, as it was initially thought they too would react well under the experimental conditions. The samples were cut from a reactive habit of pyrite and had rough surfaces with many valleys and divots – some containing rusty oxidation (Fig. 3) prior to experimentation. This in conjunction with pyrite's increased reactivity at relative humidities greater than 60% (Brunton et al. 1984: C11; Newman 1998: 367; Larkin 2001: 35), would lead one to assume a visible reaction would occur when exposed to 74%RH and 60°C. Perhaps a week's exposure was insufficient, or there was insufficient oxygen available for reaction, due to the vessels containing mostly acetic acid and sodium chloride vapour. As aforementioned, it is difficult to determine what reactions occurred and their products, yet the primary supposition is that the samples oxidised to a degree, with additional, minute yet widespread reaction with sodium chloride vapours to create sodium-containing salts (Fig. 6, 8b).

Future Research

The results from this experiment inform more on what *not* to do than what *to* do in future experiments.

Firstly, salt solutions should not be used to create humid environments. By doing so, one adds not just another variable, but in most cases an unwanted contaminant. Thicket (1997: 4) used glycerol instead of a salt solution in his experiment, so it would be worth testing glycerol’s efficacy at creating humid conditions and its effect on samples. If this method proves to be effective, then a further experiment could be devised to examine how acetic acid reacts to calcite without the interference of a soluble salt.

Secondly, colorimetry provides baseless data with uneven surfaces. This questions its application on minerals, which are often uneven. Does one need to flatten mineral surfaces in order to get an accurate reading? By doing so, would it change the optical properties of said mineral? Would the results be comparable to unprepared minerals? These question warrant their own experiment.

Thirdly, more forms of quantitative compositional analysis are needed to better understand the reaction products. While an additional two analytical methods (x-ray diffraction and FT-IR) were planned to be used at the outset of the experiment, the equipment was unavailable during the time constraints of the experiment. Consequently, reaction products were only identified by EDS, which informs one of the elemental composition. It would have been greatly helpful in product identification to have bond compositions as well, which could help narrow down possible compounds.

Finally, the accelerated aging conditions chosen were too extreme. Not only would such environments be unlikely for museums, there is no accurate way of correlating accelerated and real-time exposure, primarily due to the fact that reactions accelerate and different deterioration pathways occur at higher temperatures. How a material reacts at room temperature is often vastly different from how it would at 40°, 60°, 100°C. In addition, the concentration of acetic acid was much higher than what would be expected in typical museum conditions. In this experiment, approximately 0.14g/L or 63,733.66 ppmV (Appendix D) of acetic acid vapour were in each vessel. Common concentrations of acetic acid in wooden housing are 0.03-3 ppmv (Tétreault et al. 2003: 244), although concentrations can be higher if other acetate-containing products are used in conjunction. Thus, all variable, save for possibly humidity, vary greatly from typical museum conditions, and it would be extremely difficult to determine how this exposure would relate to dose/year in a realistic setting. Future experiments should be allowed sufficient time to run in realistic conditions (15-23°C, 45-65%RH, ≤ 5 ppmV acetic acid) in order to see results, rather than forcing them through intensifying conditions to fit a short timeframe.

Conclusion

As anticipated, quantifable data and groundbreaking insights were not produced during this experiment. In reagrds to being a proof-of-concept, the experiment proved to be inappropriate to test the effects of common gaseous pollutants on minerals. While vessel construction was sucessful at this scale, it might not be efficient or feasible with more samples. The use of a salt solution provided an unwanted contaminant. Having a high acetic acid concentration in addition to a relatively high temperature produced results which are likely to be incomparable to real-time museum situations, suggesting more realistic conditions should be used. Additional forms of analysis also need to be introduced to better understand reaction products and pathways. Only then can informative results be produced.

References

Brunton, C.H.C., Besterman, T.P., and Cooper, J.A., 1984. Guidelines for the Curation of Geological Materials: Geological Society Miscellaneous Paper No. 17.

Caracanhas Cavallari, D., Brincalepe Salvador, R., and Rodrigues da Cunha, B., 2014. Dangers to malacological collections: Bynesian decay and pyrite decay. *Collection Forum*, 28 (1–2), 35–46.

EPA, 2016. Indoor Air Unit Conversion [online]. Available from: https://www3.epa.gov/ceampubl/learn2model/part-two/onsite/doc/Indoor Air Unit Conversions.pdf [Accessed 9 Jan 2019].

Fu, H., Guan, B., Jiang, G., Yates, M.Z., and Wu, Z., 2012. Effect of supersaturation on competitive nucleation of CaSO4phases in a concentrated CaCl2solution. *Crystal Growth and Design*, 12 (3), 1388–1394.

GmbH, D., 2019. Saturated Vapor Pressure: Calculation by Antoine Equation [online]. Available from: http://ddbonline.ddbst.com/AntoineCalculation/AntoineCalculationCGI.exe [Accessed 9 Jan 2019].

Greenspan, L., 1977. Humidity Fixed Points of Binary Saturated Aqueous Solutions. *Journal of Research of the National Bureau of Standards - A. Physics and CHemistry*, 81A (1), 89–96.

Grzywacz, C.M., 2006. *Monitoring for Gaseous Pollutants in Museum Environments*.

Hu, Z. and Deng, Y., 2004. Synthesis of needle-like aragonite from calcium chloride and sparingly soluble magnesium carbonate. *Powder Technology*, 140 (1–2), 10–16.

Konica Minolta, 2019. Specular Component Included (SCI) vs. Specular Component Excluded (SCE) [online]. Available from: https://sensing.konicaminolta.us/blog/specular-component-included-sci-vs-specular-component-excluded-sce/ [Accessed 9 Jan 2019].

Larkin, N.R., 2001. Pyrite Decay : cause and effect , prevention and cure . *NatSCA News*, (21), 35–43.

Liu, L., Hu, B., Chen, S.F., Liu, S.J., Jiang, J., Cai, G. Bin, and Yu, S.H., 2010. Mineralization of calcite ribbons on an Allium fistulosum L. bulb inner membrane in an ethanol-water mixed solvent under control of polyacrylic acid by a double diffusion method. *CrystEngComm*, 12 (11), 3593–3598.

Mindat.org, T.H.I. of M. dba, 2019. Pyrite [online]. Available from: https://www.mindat.org/min-3314.html [Accessed 9 Jan 2019].

Newman, A., 1998. Pyrite Oxidation and Museum Collections: a review of theory and conservation treatments. *The Geological Curator*, 6 (10), 363–371.

Omega, n.d. Equilibrium Relative Humidity Saturated Salt Solutions.

Rautaray, D., Ahmad, A., and Sastry, M., 2004. Biological synthesis of metal carbonate minerals using fungi and actinomycetes. *Journal of Materials Chemistry*, 14 (14), 2333–2340.

Tennent, N.H. and Baird, T., 1985. The Deterioration of Mollusca Collections: Identification of Shell Efflorescence. *Studies in Conservation*, 30 (2), 73–85.

Tétreault, J., Cano, E., van Bommel, M., Scott, D.A., Dennis, M., Barthés-Labrousse, M.-G., Minel, L., and Robbiola, L., 2003. Corrosion of copper and lead by formaldehyde, formic and acetic acid vapours. *Studies in Conservation*, 48 (4), 237–250.

Thickett, D., 1997. *Relative Effects of Formaldehyde, Formic and Acetic Acids on Lead, Copper and Silver*.

Waller, R., Andrew, K.J., and Tetreault, J., 2000. Survey of Gaseous Pollutant Concentration Distributions in Mineral Collections. *Collection Forum*, 14 (1–2).

Appendixes

Appendix A. Equipment and Software Providers

Genlab Oven OV/125/F/DIG

Genlab Limited
Tanhouse Lane, Riverview Industrial Estate,
Widnes, Cheshire, WA8 0SR
Tel: +44 (0)151 424 5001
Fax: +44 (0)151 495 2197
Email: enquiries@genlab.co.uk
https://www.genlab.co.uk

Jeol 5910 SEM

JEOL (Europe) BV
Lireweg 4
2153 PH Nieuw-Vennep
The Netherlands
Phone: (31) 252 623 500
Fax: (31) 252 623 501
sales@jeolbenelux.com
https://www.jeolbenelux.com

Keyence Digital Microscope VH-250L & Keyence VHX5000

KEYENCE (UK) LIMITED
Avebury House, 219-225 Avebury Boulevard,
Milton Keynes MK9 1AU
Phone: +44 (0) 1908-696-900
ukinfo@keyence.co.uk
https://www.keyence.co.uk

Konica Minolta CM-700d Spectrophotometer & SpectraMagic NX

Konica Minolta UK Office
9 Webster Court, Westbrook Crescent
Gemini Business Park
Warrington, WA5 8WD
Phone: +44 (0)1925 467 300
Fax: +44 (0)1925 711 143
info.uk@seu.konicaminolta.eu
www.konicaminolta.com

Leica MSV269 Stereomicroscope

Leica Microsystems UK (Ltd)
Larch House, Woodlands Business Park,
Breckland, Linford Wood
Milton Keynes, MK14 6FG
Office Phone: 0800 298 2344
Service Phone: +44 845 604 9095
Fax: +44 (0)1908 577 640
www.leica-microsystems.com

Oxford Instruments INCA 300 EDA

Oxford Instruments NanoAnalysis & Asylum Research, UK
Halifax Rd, High Wycombe
HP12 3SE, UK
T: +44 (0)1494 479369
F: +44 (0)1494479369
https://nano.oxinst.com

Sartorius CP42025 digital balance

Sartorius Stedim UK Ltd.
Longmead Business Centre
Blenheim Road, Epsom
Surrey KT19 9QQ
Phone: +44.1372.737100
Fax: +44.1372.726171
ne.customersupport@sartorius-stedim.com
www.sartorius.co.uk

Appendix B. Sample Weights Before and After Deterioration

Table 2. Calcite weights ± 0.01g before & after deterioration. Changes ±0.02 are considered within the range of error.

Sample #	Weights Before Deterioration (g)			Average Weight (g)	Weights After Deterioration (g)			Average Weight (g)	Δ Weight (g)
	Weight 1	Weight 2	Weight 3		Weight 1	Weight 2	Weight 3		
1	8.68	8.69	8.69	8.69	9.00	9.01	9.01	9.01	+0.40
2	10.41	10.41	10.40	10.41	10.61	10.63	10.62	10.62	+0.21
3	9.60	9.61	9.61	9.61	9.86	9.86	9.85	9.86	+0.25
4	13.90	13.90	13.90	13.90	14.06	14.07	14.06	14.06	+0.16
5	15.83	15.82	15.82	15.82	16.10	16.09	16.09	16.09	+0.27
6	7.87	7.88	7.87	7.87	7.85	7.85	7.85	7.85	-0.02
7	11.40	11.40	11.41	11.40	11.40	11.40	11.40	11.40	-
8	10.41	10.41	10.40	10.41	10.40	10.40	10.40	10.40	-0.01
9	8.46	8.46	8.46	8.46	8.46	8.47	8.46	8.46	-
10	10.70	10.69	10.68	10.69	10.67	10.67	10.67	10.67	-0.02

Table 3. Pyrite weights ± 0.01g before & after deterioration. Changes ±0.02 are considered within the range of error.

Sample #	Weights Before Deterioration (g)			Average Weight (g)	Weights After Deterioration (g)			Average Weight (g)	Δ Weight (g)
	Weight 1	Weight 2	Weight 3		Weight 1	Weight 2	Weight 3		
1	3.46	3.46	3.46	3.46	3.45	3.46	3.46	3.46	-
2	2.13	2.14	2.14	2.14	2.14	2.14	2.13	2.14	-
3	3.48	3.47	3.48	3.48	3.48	3.48	3.48	3.48	-
4	3.09	3.09	3.09	3.09	3.10	3.10	3.09	3.10	+0.01
5	4.16	4.16	4.16	4.16	4.16	4.17	4.16	4.16	-
6	4.75	4.74	4.74	4.74	4.74	4.75	4.74	4.74	-
7	2.67	2.68	2.67	2.67	2.67	2.68	2.67	2.67	-
8	3.74	3.75	3.75	3.75	3.74	3.75	3.74	3.74	-0.01
9	4.47	4.48	4.47	4.47	4.47	4.48	4.47	4.47	-
10	3.10	3.09	3.09	3.09	3.09	3.09	3.09	3.09	-
11	2.86	2.86	2.86	2.86	2.84	2.85	2.85	2.85	-0.01
12	3.59	3.60	3.59	3.59	3.59	3.60	3.59	3.59	-
13	5.00	5.04	5.03	5.02	5.03	5.03	5.02	5.03	+0.01
14	3.24	3.23	3.23	3.23	3.23	3.23	3.23	3.23	-
15	4.97	4.97	4.97	4.97	4.96	4.97	4.96	4.96	-0.01
16	4.90	4.89	4.88	4.89	4.89	4.88	4.88	4.88	-0.01
17	4.77	4.77	4.77	4.77	4.78	4.78	4.78	4.78	+0.01
18	3.28	3.29	3.28	3.28	3.30	3.29	3.29	3.29	+0.01
19	3.45	3.45	3.45	3.45	3.45	3.45	3.45	3.45	-

Appendix C. Colour and Lightness Measurements Before and After Deterioration

Table 4. Colour & lightness measurements (SCE) of calcite samples, before and after deterioration, as well as the degree of change

Sample #		L*(D65)	a*(D65)	b*(D65)	C*(D65)	h(D65)
C1	Before	46.86	1.25	4.66	4.82	74.98
	After	82.12	0.19	0.82	0.84	76.66
	Δ	35.26	-1.06	-3.84	-3.98	0.06
C2	Before	62.95	-0.01	1.54	1.54	90.27
	After	79.92	-0.01	1.56	1.56	90.22
	Δ	16.34	0	0.02	0.02	0
C3	Before	58.60	1.49	6.84	7	77.71
	After	79.64	1.21	7.91	8	81.31
	Δ	21.05	-0.28	1.07	1	0.47
C4	Before	53.68	0.63	5.76	5.80	83.77
	After	74.11	1.12	6.91	7	80.79
	Δ	20.43	0.49	1.15	1.20	-0.33
C5	Before	56.82	-0.38	1.87	1.91	101.35
	After	89.45	0.03	1.06	1.06	88.38
	Δ	32.63	0.41	-0.81	-0.85	-0.32
C6	Before	54.30	0.19	3.24	3.24	86.63
	After	35.70	0.21	1.80	1.81	83.42
	Δ	-18.60	0.02	-1.43	-1.43	0.97
C7	Before	46.16	1.37	8.79	8.90	81.16
	After	41.71	-0.05	3.76	3.76	90.81
	Δ	-4.45	-1.42	-5.04	05.14	0.97
C8	Before	60.42	0.40	4.97	4.99	85.41
	After	52.84	0.48	4.68	4.71	84.13
	Δ	-7.58	0.08	-0.29	-0.28	-0.11
C9	Before	59.24	-0.45	4.55	4.58	95.69
	After	47.95	-0.22	3.66	3.67	93.36
	Δ	-11.29	0.24	-0.89	-0.91	-0.17
C10	Before	57.00	-0.05	1.04	1.04	92.67
	After	46.19	0.02	1.01	1.01	88.79
	Δ	-10.81	0.07	-0.05	-0.05	-0.07

Table 5. Colour & lightness measurements (SCE) of pyrite samples, before and after deterioration, as well as the degree of change.

Sample #		L*(D65)	a*(D65)	b*(D65)	C*(D65)	h(D65)
P1	Before	57.36	-0.25	9.01	9.01	91.59
	After	33.49	0.21	9.16	9.16	88.69
	Δ	-23.87	0.46	0.15	0.14	-0.46
P2	Before	32.77	-0.27	-3.16	3.17	265.09
	After	57.96	0.24	11.77	11.77	88.85
	Δ	25.19	0.51	14.93	8.59	-12.22
P3	Before	59.46	-0.30	9.25	9.25	91.84
	After	52.23	0.60	12.28	12.29	87.18
	Δ	-7.23	0.90	3.03	3.04	-0.87
P4	Before	59.69	-0.32	8.72	8.73	92.08
	After	56.54	-0.10	9.61	9.61	90.59
	Δ	-3.15	0.22	0.89	0.89	-0.24
P5	Before	61.49	-0.24	9.63	9.63	91.45
	After	25.22	-0.24	-4.38	4.39	266.83
	Δ	-36.27	0	-14.01	-5.25	12.99
P6	Before	61.34	-0.24	9.93	9.93	91.38
	After	60.68	-0.31	9.70	9.71	91.84
	Δ	-0.66	-0.07	-0.22	-0.22	0.08
P7	Before	60.86	-0.29	9.45	9.46	91.74
	After	52.13	0.09	9.60	9.60	89.45
	Δ	-8.73	0.38	0.15	0.14	-0.38
P8	Before	55.82	-0.19	9.58	9.58	91.11
	After	24.30	-0.15	-3.96	3.96	267.82
	Δ	-31.52	0.03	-13.54	-5.62	12.32
P9	Before	59.48	-0.18	9.22	9.22	91.11
	After	39.64	-0.02	6.35	6.35	90.16
	Δ	-19.84	0.16	-2.87	-2.87	-0.13
P10	Before	60.67	-0.22	9.54	9.55	91.30
	After	55.24	-0.26	8.73	8.73	91.71
	Δ	-5.42	-0.05	-0.81	-0.81	0.07
P11	Before	57.5	-0.17	9.33	9.33	91.04
	After	33.51	1.03	7.38	7.46	82.08
	Δ	-23.99	1.20	-1.94	-1.88	-1.30
P12	Before	55.63	-0.31	8.97	8.97	92
	After	31.15	-0.04	-0.45	0.45	265.05
	Δ	-24.47	0.27	-9.42	-8.52	4.02

Note: SCE (specular component excluded) measurements – and not SCI (specular component included) measurements - were provided, as SCE best reflects how humans see a colour, rather than its ‘true’ colour (Konica Minolta 2019). While there is a difference between the two data sets, it is slight and the inclusion of both would be overwhelming while producing little additional insight.

Appendix D. Equations and Calculations

Referencing Thickett 1997, equation (1) was used to determine the partial vapour pressure of the acetic acid vapour.

$$C_{vap} = \frac{\frac{m_a}{M_a}}{(\frac{m_a}{M_a}+\frac{m_b}{M_b})} \left(C^{\circ}{}_{vap}\right) \qquad \textbf{\textit{(1)}}$$

Where: C_{vap} – pressure of vapour above the solution
m_a – mass (g) of phase ‘a’ in solution (phase giving rise to the vapour; acetic acid in this case)
M_a – relative molecular mass (g/mol) of phase ‘a’
m_b – mass (g) of phase ‘b’ in solution (water in this case)
M_b – relative molecular mass (g/mol) of phase ‘b’
$C°_{vap}$ – pressure of pure vapour phase ‘a’

In order to calculate $C°_{vap}$, Thickett (1997: 13) used equation (2):

$$\log C^{\circ}{}_{vap} = A - \frac{1}{BT} \qquad \textbf{\textit{(2)}}$$

Where: T – temperature
A, B – constants dependant on species

For acetic acid, Thickett (1997: 13) documents the constants as: A = 8.319, B = 0.00047

However, the author was unable to receive a reasonable answer using equation (2), producing $10^{4.773}$, an unreasonably large number. This equation, referenced by Thickett to be from Atkins’ 2nd edition of *Physical Chemistry*, is thought to be a derivative of the Clausius–Clapeyron vapour pressure equation, but is an undocumented one. Hence an alternate vapour pressure equation was used, the Antoine Equation (3), and was found successful.

$$P = 10^{A - \frac{B}{C+T}} \tag{3}$$

Where: P – vapour pressure (mmHg) of pure species
A,B,C – constants dependant on species (Table 6)
T – temperature (°C)

Table 6. Antoine Equation parameters for acetic acid (GmbH, D., 2019)

T_{min} (°C)	T_{max} (°C)	A	B	C
17	118	7.5596	1644.05	233.524
118	227	8.26735	2258.22	300.97

Using equation (3) and the appropriate constants (Table 6), the calculated value for the vapour pressure of a 100% solution of acetic acid was 90.89 mmHg. This value was verified by DDBST's online calculator (GmbH, D., 2019). It was then inserted into equation (1), producing the partial vapour pressure of 50.90 mmHg.

In order to determine the concentration in parts per million volume (ppmV), the quantity of acetic acid vapour had to first be calculated through the Ideal Gas Law (4):

$$PV = nRT \tag{4}$$

Where: P – pressure (Pa)
V – volume of vessel (m^3)
n – amount of compound (mol)
R – gas constant (8.314472 Pa(m^3)/(mol)K)
T – temperature (°K)

The equation was solved for 'n', resulting in 0.0012 mol. This value was multiplied by acetic acid's relative molecular mass to determine the mass (g) of acetic acid vapour: 0.07g/500ml or 0.14g/L.

The latter value was converted into mg/L (140mg/L) and inserted into equation (5) to determine the concentration as ppmV (EPA 2016):

$$\text{ppmV} = \frac{RTx(10^3)}{MP} \tag{5}$$

where: R – gas constant (8.314472 Pa(m^3)/(mol)K)
x – mg/L of gaseous pollutant
T – temperature of air (K)
M – relative molecular mass of gaseous pollutant (g/mol)
P – pressure of air (kPa)